minerals

MDPI

Article

Large Amount of Excess Argon in Hydrothermal Quartz from the Vangtat Orogenic Gold Belt, Southern Laos: New In-Sight from K-Ar and Noble Gas Isotope Analyses

Patthana Bounliyong [1,*], Hirochika Sumino [2] and Antonio Arribas [3]

[1] Center of Regional Revitalization in Research and Education, Akita University, Akita 010-8502, Japan
[2] Research Center for Advanced Science and Technology, University of Tokyo, Tokyo 153-0041, Japan
[3] Department of Earth, Environmental and Resource Sciences, The University of Texas at El Paso, El Paso, TX 79986, USA
* Correspondence: to.geology@gmail.com

Abstract: K-Ar dating and $^{3}He/^{4}He$ and $^{40}Ar/^{36}Ar$ analyses were conducted on samples of hydrothermal quartz from the Thongkai-Ok Au deposit in the Vangtat orogenic Au belt of southern Laos to study the presence of excess argon in hydrothermal quartz and to better understand the origin of the ore-forming fluids. The K-Ar age of two hydrothermal quartz separates yielded apparent dates of 1040 and 1385 Ma. These ages are significantly older than the estimated age of Vangtat Au mineralization (~200 Ma) and other regional geologic events, indicating the presence of an extraordinary amount of excess argon in the hydrothermal quartz crystals. In vacuo crushing analyses of the Thongkai-Ok hydrothermal vein quartz delivered $^{3}He/^{4}He \approx 0.2–0.3$ R/Ra and $^{40}Ar/^{36}Ar \approx 455–725$, suggesting the ore-forming fluid is mainly derived from a crustal component with a minor contribution of mantle and meteoric fluids.

Keywords: noble gas isotopes; in vacuo crushing method; hydrothermal quartz; Thongkai-Ok; Vangtat; excess argon

Citation: Bounliyong, P.; Sumino, H.; Arribas, A. Large Amount of Excess Argon in Hydrothermal Quartz from the Vangtat Orogenic Gold Belt, Southern Laos: New In-Sight from K-Ar and Noble Gas Isotope Analyses. *Minerals* **2022**, *12*, 1205. https://doi.org/10.3390/min12101205

Academic Editor: David Phillips

Received: 13 August 2022
Accepted: 21 September 2022
Published: 24 September 2022

1. Introduction

K-Ar ($^{40}Ar/^{39}Ar$) analyses of phengitic micas from metamorphic rocks in many orogenic belts have yielded discordant and geologically meaningless ages (cf. Itaya, 2020 [1] and references therein). This is due to the fact that white micas in continental lithologies consisting of precursor older rocks have not been reset completely during *MP–HP–UHP* metamorphism because of the high closure temperature (ca. 600 °C) of white mica (cf. Itaya, 2020 [1] and references therein). Biotite also has complex excess Ar behavior in thermally overprinted rocks near tectonic boundaries [2] and/or in contact aureoles [3]. This type of excess ^{40}Ar was incorporated into biotite by diffusion. This phenomenon was later named "Excess-Argon Wave" [4,5] and has been observed in kyanite and K-feldspar [6,7].

In a recent study of Au mineralization in the Vangtat orogenic Au belt of southern Laos [8], Bounliyong et al. (2021) [9] dated samples of hydrothermal muscovite from the shear-zone hosted quartz veins of the Thongkai-Ok Au deposit. The K-Ar ages of four size fractions (<2, 2–4, 4–10, and 10–40 μm) separated from three hydrothermal muscovite samples revealed a large range of calculated ages, from 348 to 206 Ma [9]. This age range was found to correlate well with the amount of quartz present in the sample separates as a mineral impurity. Bounliyong et al. (2021) [9] concluded that the coarser-grained samples, which contained a larger amount of quartz and had a corresponding lower K content (2–4 wt%), gave older dates (350 to 280 Ma); whereas the finer-grained samples, which contained fewer quartz impurities and had a high K content (6–8 wt% K), resulted in the youngest K-Ar dates (e.g., 206 ± 4 Ma), which were interpreted to be closest to the age of mineralization. The large range of calculated ages was hypothesized to reflect excess

Ar contained in the hydrothermal vein quartz, most likely in fluid inclusions in the quartz crystals [9]. Such an interpretation is consistent with previous studies [10–14]. However, the mechanism of how the excess Ar incorporates into hydrothermal quartz is still vague. To better understand the presence of excess argon in the Vangtat orogenic Au deposit and its potential origin, in this study we conducted (i) K-Ar dating analyses and fluid inclusion measurements on pure hydrothermal vein quartz; and (ii) Ar and He isotope analyses of fluid inclusions in quartz e.g., [15,16].

2. Background Geology

2.1. Regional Geology

The Vangtat shear zone is the structural host for the Vangtat orogenic Au belt in southern Laos (Figure 1) [8]. The Vangtat shear zone is the main subsidiary structure of the Poko suture zone (PKSZ, Figure 1), which resulted from the collision between the Indochina Terrane and the Kontum Massif during the Permo-Triassic [17–20]. Known Au mineralization in this region is associated with regional metamorphism and is mainly distributed along the Poko suture zone and the Tam Ky-Phuoc Son suture zone in the northern flank of the Kontum Massif. The timing of Au mineralization is related to the late stage of the Indosinian Orogeny (c.a., 250 to 200 Ma) [9,21,22].

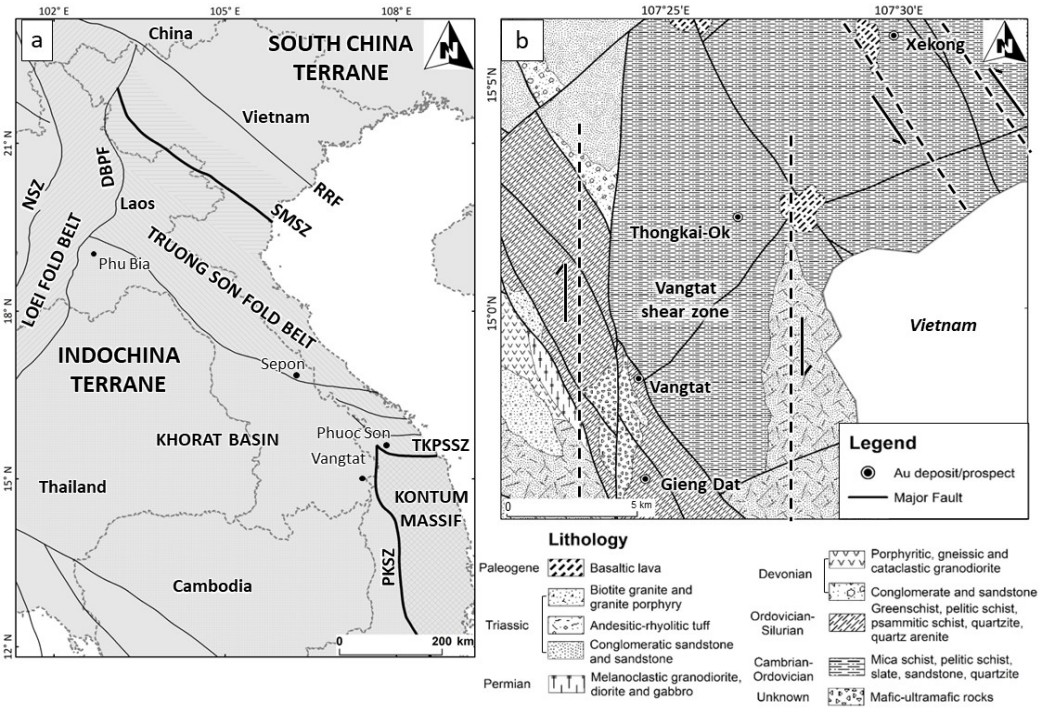

Figure 1. (**a**) Main tectonic terranes and domains of mainland Southeast Asia, and associated metal deposits (mod. From Lepvrier et al. (2008) [17]). Abbreviations: DBPF: Dien Bien Phu Fault; NSZ: Nan Suture Zone; PKSZ: Poko Suture Zone; RRF: Red River Fault; SMSZ: Song Ma Suture Zone; TKPSSZ: Tam Ky-Phuoc Son Suture Zone. (**b**) Geological map of the Vangtat shear zone, southeastern Laos, and the distribution of Au deposits (Bounliyong et al. (2021) [9]; after Vilayhack et al. (2008) [18]). The black dashed lines roughly mark the boundaries of the shear zones.

2.2. Deposit Geology and Mineralization

The Thongkai-Ok Au deposit is one of several actively mined deposits in the newly discovered Vangtat orogenic Au belt of southern Laos [9]. The major orebodies within the high-grade belt are found in quartz-sulfide-carbonate-graphite-white mica-chlorite veins in which Au is commonly present as inclusions within sulfides, mainly pyrite [8]. The quartz veins and silicified zones have a thickness of up to 10 m and are hosted by strongly deformed and sheared pelitic schist [8]. Lower-grade Au mineralization occurs in

a graphite-carbonate-quartz-sulfide alteration envelope that grades into sub-economic to barren altered pelitic schist [8].

3. Sample Preparation

For this research, two samples of hydrothermal vein quartz (TKO-1 and 20190404-5) out of the three samples studied by Bounliyong et al. (2021) [9] were chosen for K-Ar and noble gas isotope analyses. The samples were collected from the main Au veins being mined and are considered to be representative of the Thongkai-Ok Au mineralization [9]. Quartz vein samples were broken down in a stainless-steel mortar and pestle and cleaned with distilled water. Quartz fractions between 0.25 and 1 mm in diameter were picked clean under the binocular microscope (Figure 2a). These quartz fractions were further gently crushed in the agate mortar and pestle and the impurity particles (e.g., clay minerals, fine-grained pyrite) were excluded. The pure fractions were cleaned with distilled water using an ultrasonic bath.

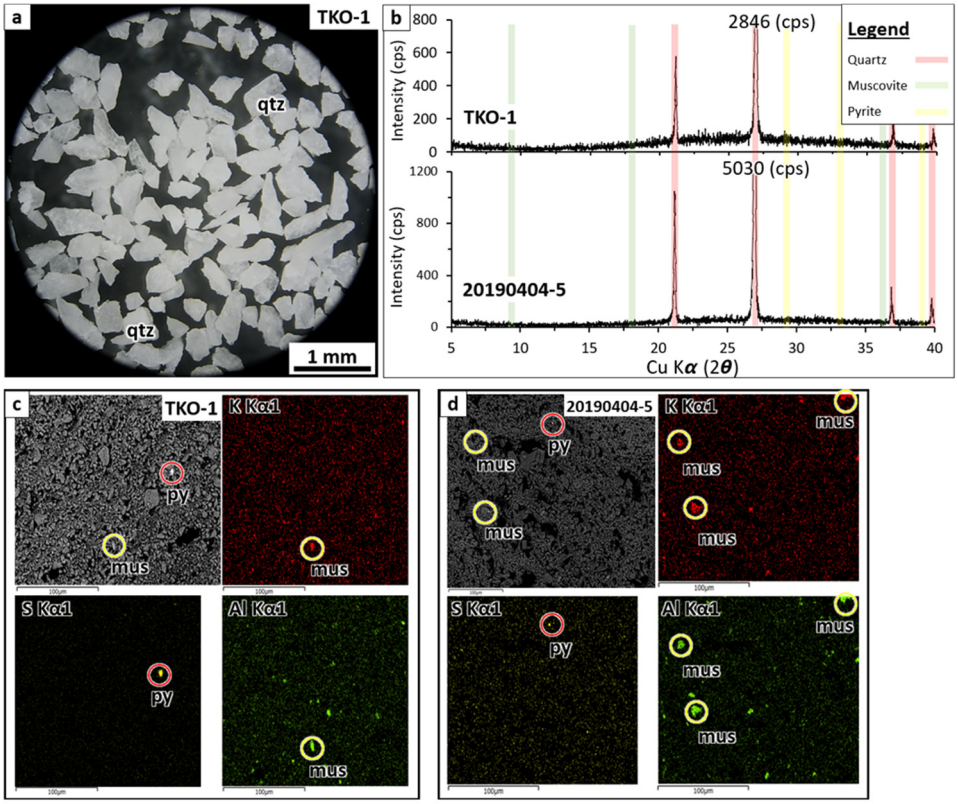

Figure 2. (**a**) Photo of quartz separate fractions; (**b**) X-ray diffraction patterns of quartz separate samples; (**c**,**d**) elemental mapping of quartz separate samples under a scanning electron microscope showing the negligible impurities of associated minerals, such as muscovite (mus) and pyrite (py).

To test the purity of the quartz separates, X-ray diffraction (XRD) spectra were collected using a Rigaku Multiflex X-ray diffractometer with a Cu-Kα tube (30 kV, 16 mA, receiving slit = 0.3 mm, step = 0.01, 2° 2θ/min) at Akita University. The results show almost pure quartz (Figure 2b). In addition, the quartz separates were observed under a scanning electron microscope (SEM), using a JOEL JSM-6610 LV SEM (15 kV, ~2.2 nA, 10.0 mm WD) with an Oxford Instruments INCA X-act energy-dispersive spectrometer detector. The SEM images allowed the identification of trace amounts of white mica and pyrite contained in the quartz separates (Figure 2c,d).

4. Fluid Inclusion Microthermometry

Fluid inclusion microthermometric measurements were conducted on doubly polished thick sections (150 to 300 μm) of quartz samples, using a Linkam 10035 freezing and heating stage at Akita University. Temperatures were calibrated using the melting temperatures of the following components: CO_2 liquid (−56.6 °C), n-dodecane (−9.6 °C), n-tridecane (−5.5 °C), pure water (0 °C), n-tetradecane (+5.5 °C), benzanilide (+163 °C), sodium nitrate (+308 °C), potassium dichromate (+398 °C), and cupric chloride (+498 °C). The errors from the measurements of the standard materials are less than 0.1 °C.

The fluid inclusions assemblages (FIAs) observed in quartz crystals from the mineralized veins of the Thongkai-Ok Au deposit appear as isolated groups of fluid inclusions (Figure 3a), which are commonly considered as primary in origin [23], although there is always some uncertainty about the ultimate primary, secondary, or pseudo-secondary origin of fluid inclusions [24]. Most of the studied fluid inclusions are tiny in size, commonly less than 10 μm, regular in shape, and dominantly liquid-rich or two-phase liquid-vapor inclusion (Figure 3b).

The results of the microthermometric study of FIAs from the Thongkai-Ok deposit are summarized in Table 1. All the fluid inclusions studied homogenized to the liquid phase, and the majority of fluid inclusions exhibited a narrow range of homogenization temperature (T_h) and salinity: 184 to 230 °C and 0.7 to 5.2 wt% NaCl equivalent (avg. = 3.0 wt% NaCl equiv.; Figure 3c), respectively (Table 1; salinity calculations based on the equation of Bodnar, 1993 [25]). The plotted data of homogenization temperature and salinity suggest an isothermal mixing trend for the hydrothermal fluids (Figure 3d) [26]. The microthermometric data from the fluid inclusions from the Thongkai-Ok Au deposit are consistent with those from fluid inclusions in hydrothermal quartz from the Au-bearing veins at the main Vangtat Au deposit (e.g., homogenization temperature: 240–250 °C and salinity: 4–6 wt% NaCl equivalent; Bounliyong et al., 2022), located some 8 km to the SW (Figure 1).

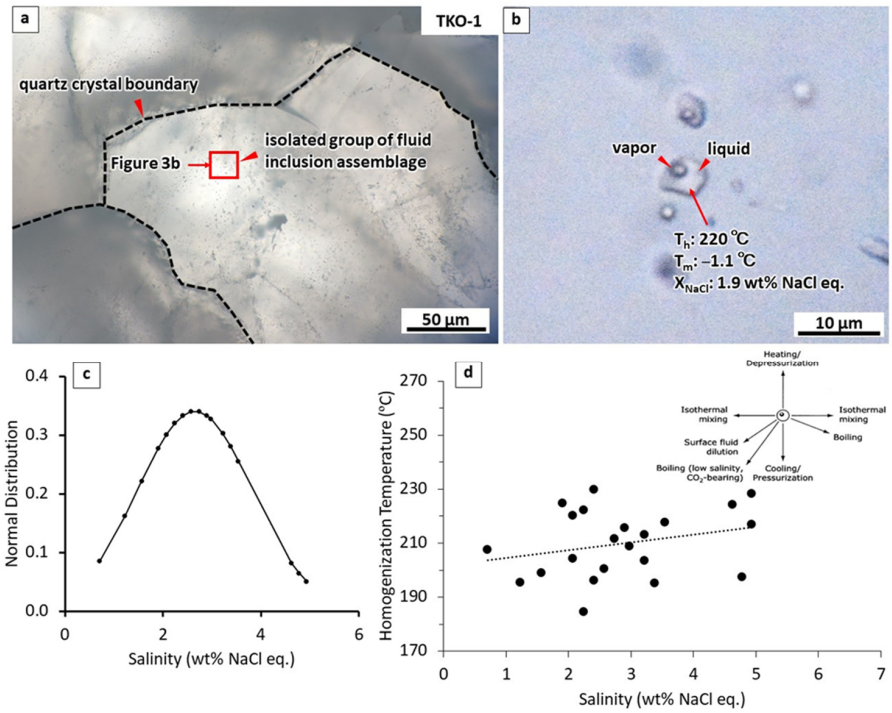

Figure 3. (**a**) Photomicrographs showing the fluid inclusion assemblages inside quartz crystals from the Thongkai-Ok Au deposit; (**b**) two-phase liquid-vapor inclusions; (**c**) graph showing normal distribution of fluid inclusion salinity; (**d**) correlation diagram of homogenization temperature (T_h) vs. salinity, the typical trend in Th-salinity from Wilkinson (2001) [26].

Table 1. Summary of microthermometry of fluid inclusions trapped in vein quartz from the Thongkai-Ok deposit.

Location	Inclusion Phase	Inclusion Size (μm)	Number of Fluid Inclusions	Tm_{ice} (°C)	Th_{total} (°C)	Salinity (wt% NaCl)
Thongkai-Ok	L>V	5–10	22	–0.4 to –3.2	184–230	0.7–5.2

5. Potassium-Argon Analyses

The K-Ar analyses were performed at the laboratories of the Okayama University of Science. Potassium concentrations in the quartz separates were determined with the low-K analytical method developed by Itaya et al. (1996) [27], using a newly designed and constructed ultra-low blank chemical line. Multiple runs of a standard (JP-1, 0.00387 wt %) [27] indicate that the error of the analyses is less than 5%. However, we assigned an error of 5% to the K measurements of the quartz separates. Argon isotopes were analyzed with a 15 cm radius sector-type mass spectrometer with a single collector, utilizing isotope dilution and ^{38}Ar spike methods [28]. Mass discrimination was checked with atmospheric Ar several times each day. Quartz separates wrapped in Al foil were vacuumed out at 150–200 °C for two days, and Ar isotopes were then extracted at 1500 °C in an ultra-high vacuum line. Reactive gases were removed using a Ti-Zr scrubber. The decay constants for ^{40}K to ^{40}Ar and ^{40}Ca, and ^{40}K content in K used in the age calculation, are 0.581×10^{-10}/y, 4.962×10^{-10}/y, and 0.0001167, respectively [29]. The errors for the ages are at a two-sigma confidence level.

The results of K-Ar analyses of quartz separates and age calculations are shown in Table 2. The samples 20190404-5 and TKO-1 give apparent ages of 1040 and 1385 Ma, respectively. These ages are significantly older than the age of Au mineralization in the Vangtat orogenic Au belt (~200 Ma) [9] and the peak metamorphic event in the Kontum Massif (270 Ma) [20]. The results indicate a very large amount of excess Ar in the hydrothermal vein quartz.

Table 2. K-Ar dating results for quartz samples from the Thongkai-Ok deposit.

Sample	Mineral	K Content (wt%)	Rad. ^{40}Ar (10^{-8} cc STP/g)	K-Ar Age (Ma)	Non-Rad. ^{40}Ar (%)
TKO-1	Quartz	0.0455 ± 0.0023	367.8 ± 4.7	1385 ± 50	21.3
20190404-5	Quartz	0.0594 ± 0.0030	324.1 ± 4.4	1040 ± 41	25.6

6. Noble Gases Isotope Analyses

The isotopic ratios (^{3}He/^{4}He, ^{20}Ne/^{22}Ne, ^{21}Ne/^{22}Ne, ^{38}Ar/^{36}Ar, and ^{40}Ar/^{36}Ar) and abundances of major isotopes (^{4}He, ^{20}Ne, ^{40}Ar, ^{84}Kr, and ^{132}Xe) of noble gases were measured with a sector-type mass spectrometer, a modified-VG5400 (MS-IV) at the University of Tokyo. Seven stainless-steel tubes with metal valves were connected to a noble gas purification line. The quartz separates, weighing ca. 1 g each, and Ni rods were separately installed in each tube. The quartz separates were pumped overnight at room temperature under an ultra-high vacuum to remove atmospheric noble gas contamination. Noble gas isotopes were extracted from the quartz separates using in vacuo crushing method developed by Sumino et al. (2001) [30]. In the crushing experiments, the quartz separates were crushed in the stainless-steel tube by 500 strokes of the Ni rod driven from outside the vacuum by a solenoid magnet. The gases were released by an additional 2000 strokes carried out after analysis of the first crushing step. During the crushing of a sample, the metal valves for other samples were closed to avoid cross-contamination among samples. The crushed sample was collected and a heating experiment at 1800 °C was conducted, and isotopic compositions of the released noble gases were measured.

Sensitivities and discrimination factors for noble gas isotopes, except for ^{3}He/^{4}He, were determined by measuring known amounts of atmospheric gas. The mass discrimi-

nation factor for $^{3}He/^{4}He$ ratio was determined using the He Standard of Japan (HESJ), with $^{3}He/^{4}He = (28.88 \pm 0.14) \times 10^{-6}$ [31]. Blank levels, measured using an empty tube with the same procedure applied to samples, were 3.5×10^{-11} (^{4}He), 3.9×10^{-12} (^{20}Ne), 5.7×10^{-9} (^{40}Ar), 3.7×10^{-13} (^{84}Kr), and 1.0×10^{-13} (^{132}Xe) in units of $cm^{3}STP$.

The measurement results of noble gas extraction from the two analytical methods (i.e., in vacuo crushing and heating) are shown in Table 3. Experimental uncertainties in the noble gas concentrations were estimated to be about 5% for ^{4}He and ^{40}Ar, and 10% for ^{20}Ne, ^{84}Kr, and ^{132}Xe, respectively, based on the reproducibility of measurements of a standard air sample stored in a metal container attached to the purification line. Errors on isotopic ratios incorporate errors in blank correction and mass discrimination, and are quoted at one standard deviation.

The isotopic ratios of $^{20}Ne/^{22}Ne$, $^{21}Ne/^{22}Ne$, and $^{38}Ar/^{36}Ar$ are the same as the atmospheric values (Table 3), suggesting these isotopes were possibly trapped in quartz-forming hydrothermal fluid in equilibrium with the atmosphere. However, the $^{3}He/^{4}He$ ratios (R/Ra) are significantly lower than the atmospheric value (R/Ra = 1, where $Ra = 1.4 \times 10^{-6}$) and significantly high compared to the ratio (R/Ra = 0.01–0.02) of crustal rocks [32], suggesting the existence of a mantle component. It is noted that the $^{3}He/^{4}He$ ratio of the final total fusion step is similar to that of crustal rocks, indicating the contributions of ^{4}He formed by the decay of U and Th, and ^{3}He formed by a nuclear reaction ^{6}Li (n, α)$^{3}H(\beta)^{3}He$ that exists as an impurity in quartz crystals.

The results obtained indicate that Ar isotopic ratios ($^{40}Ar/^{36}Ar$) become increasingly larger from the first to the second crushing step (from 500 to 2000 strokes) during in vacuo crushing, and significantly increase in the total fusion of crushed powder. This suggests a significant contribution of radiogenic ^{40}Ar from the decay of ^{40}K contained in white mica as an impurity in quartz (see Figure 2) versus ^{40}Ar from K in fluid inclusions.

Table 3. Noble gas isotopic composition of quartz separate sample from the Thongkai-Ok deposit, the Vangtat orogenic Au belt.

Sample	Weight (g)	Isotopic Ratios					Concentration							
		$^{3}He/^{4}He$	$^{20}Ne/^{22}Ne$	$^{21}Ne/^{22}Ne$	$^{38}Ar/^{36}Ar$	$^{40}Ar/^{36}Ar$	^{3}He	^{4}He	^{20}Ne	^{36}Ar	^{40}Ar	^{84}Kr	^{132}Xe	$F^{4}He$
		R/Ra					(10^{-15} ccSTP/g)	(10^{-9} ccSTP/g)	(10^{-11} ccSTP/g)	(10^{-8} ccSTP/g)		(10^{-12} ccSTP/g)	(10^{-13} ccSTP/g)	
TKO-1 (CR1)	0.9088	0.215 ± 0.022	9.831 ± 0.018	0.02916 ± 0.00034	0.18778 ± 0.00052	601.7 ± 0.1	1.61	5.36 ± 0.27	118 ± 12	0.204	123.0 ± 6.2	55.7 ± 5.4	31.8 ± 3.2	15.84
TKO-1 (CR2)		0.212 ± 0.027	9.823 ± 0.016	0.02910 ± 0.00044	0.1890 ± 0.0015	725.2 ± 1.4	1.07	3.61 ± 0.18	56.6 ± 5.7	0.088	63.9 ± 3.2	23.9 ± 2.4	13.9 ± 1.5	24.76
TKO-1 (H)	0.3295	0.00827 ± 0.0008	9.739 ± 0.022	0.02916 ± 0.00039	0.18750 ± 0.00094	1198.7 ± 5.4	7.17	619 ± 31	404 ± 41	0.420	504 ± 25	102 ± 11	63.4 ± 6.8	889.55
20190404-5 (CR1)	0.9325	0.311 ± 0.051	9.799 ± 0.017	0.02897 ± 0.00034	0.18793 ± 0.0007	455.1 ± 0.7	1.05	2.42 ± 0.12	125 ± 13	0.241	110.0 ± 5.5	61.7 ± 6.2	27.8 ± 3.5	6.05
20190404-5 (CR2)		0.217 ± 0.029	9.801 ± 0.015	0.02901 ± 0.00030	0.18804 ± 0.00082	594.6 ± 1.5	1.35	4.44 ± 0.22	161 ± 16	0.220	131.0 ± 6.6	53.7 ± 5.4	26.5 ± 3.4	12.18
20190404-5 (H)	0.3099	0.0191 ± 0.0013	9.762 ± 0.015	0.02923 ± 0.00036	0.1881 ± 0.001	1088.2 ± 6.4	5.56	208 ± 10	328 ± 34	0.414	451 ± 23	101 ± 11	103 ± 11	303.25
AIR		1	9.8	0.029	0.188	296								

Notes: CR1: crushing 500 strokes. CR2: crushing 2000 strokes. H: total fusion of crushed powder. R/Ra: $(^{3}He/^{4}He)_{sample}/(^{3}He/^{4}He)_{air}$; where $(^{3}He/^{4}He)_{air} = 1.4 \times 10^{-6}$.

7. Discussion

The calculated fraction of ^{3}He (from the total ^{3}He amount) obtained by the in vacuo crushing method is 27% for the TKO-1 sample and 30% for the 20190404-5 sample (see Table 3). Assuming that there was no Li-derived ^{3}He in the quartz crystals, i.e., all ^{3}He was hosted in fluid inclusions, 27%–30% of the fluid inclusions were crushed in the 2500 stroke experiment. If there was some amount of Li-derived ^{3}He in the quartz crystals, the estimated amount of fluid inclusions crushed during the crushing experiment should be higher. A similar calculation does not allow estimating the amount of ^{40}Ar release because multiple Ar components would be involved in crush-released and heating-released Ar. Although the crush-released Ar is predominantly extracted from fluid inclusions, the noticeable increase in $^{40}Ar/^{36}Ar$ ratios in the second crushing step, compared to that of the first step, indicates that there was some contribution of surface-absorbed atmospheric Ar in the first step. The results of total fusion experiments suggest that, in addition to Ar in fluid inclusions, the extracted gas contained radiogenic ^{40}Ar in quartz crystals as well as atmospheric Ar, which adsorbed on the surface of the crushed sample powder.

The Vangtat shear zone is made up of regional metamorphic rocks including schist, slate, meta-sandstone, quartzite, and quartz arenite (Figure 1b) [18]. If the hydrothermal alteration of the metamorphic rocks along the shear zone is related to the formation of the mineralized quartz veins at the Thongkai-Ok Au deposit, as proposed by Bounliyong et al. (2022) [8], the hydrothermal fluid could incorporate an "excess argon wave" similar to that proposed to explain the origin of excess Ar-bearing phengites in the Sanbagawa eclogite [5]. According to Itaya and Tsujimori (2015) [5], fluid exchange between deep-subducted sediments and mantle material led to a high Ar-pressure environment and trapping of a large amount of excess Ar within phengitic micas. The hydrothermal quartz in the Vangtat shear zone would trap the "excess argon wave" during its crystallization. As discussed in the next section, the excess Ar is predominantly concentrated in the fluid inclusions, resulting in the apparent old K-Ar ages.

Implications for the Origin of the Ore-Forming Fluids and Host of the Excess Ar

The isotopic composition of noble gases is commonly used as a sensible tracer for the origin of ore-forming fluids [33–35]. According to previous studies [16,34,35], there are three possible sources of noble gases trapped in fluid inclusions, notably: (1) mantle-derived component, $^{3}He/^{4}He \approx 8.5$ Ra and $^{40}Ar/^{36}Ar$ = 30,000 to 40,000; (2) crustal origin, $^{3}He/^{4}He$ 0.01–0.05 Ra, and $^{40}Ar/^{36}Ar$ = 299 to 100,000; and (3) atmospheric component, which is derived from air-saturated water involved in a groundwater flow system, $^{3}He/^{4}He$ = 1 and $^{40}Ar/^{36}Ar$ = 299.

The $^{40}Ar/^{36}Ar$ values within fluid inclusions of quartz separates from the Thongkai-Ok deposit obtained by in vacuo crushing experiments (455–725) are significantly lower than crust-originated fluids but higher than atmospheric $^{40}Ar/^{36}Ar$ values (Table 3). A $^{3}He/^{4}He$ (R/Ra) versus $^{40}Ar/^{36}Ar$ plot (Figure 4a) shows these relations as well as a shift for the Thongkai-Ok fluids away from the modified air-saturated water trend line [34]. The implication is that atmospheric He and/or meteoric water appear to play a negligible role in the ore-forming fluid and Au mineralization of the Thongkai-Ok Au deposit.

Atmospheric He contribution can be determined from the $F^{4}He$ values, defined as the $^{4}He/^{36}Ar$ of samples' relation to the atmospheric $^{4}He/^{36}Ar$ value of 0.1655, according to which the samples containing air will have an F-value of 1 [15]. The $F^{4}He$ values of the Thongkai-Ok quartz separates are >6 (Table 3), indicating that ^{4}He is enriched more than 6 times over the atmospheric gas.

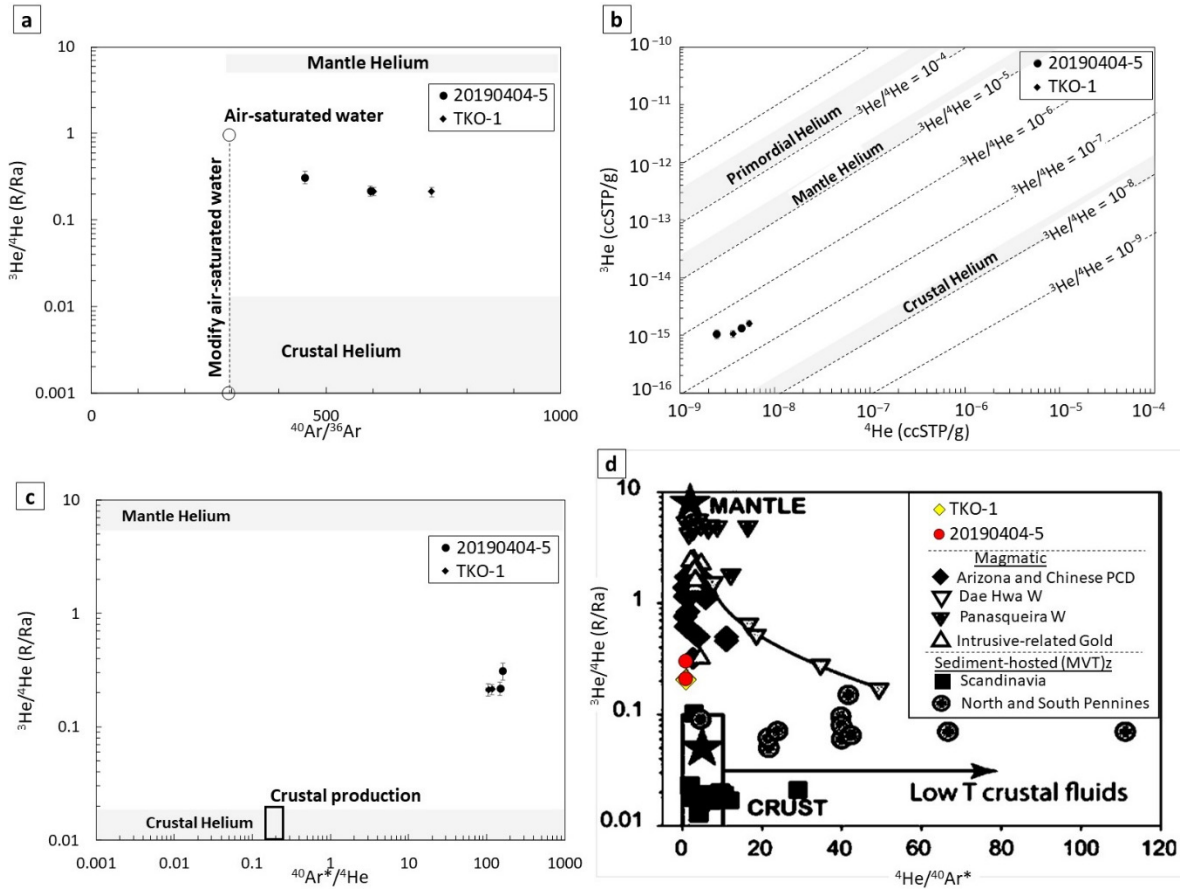

Figure 4. Correlation diagrams of noble gas isotopic composition from fluid inclusions trapped inside quartz separate samples at the Thongkai-Ok Au deposit: (**a**) plot of $^{3}He/^{4}He$ (R/Ra) vs. $^{40}Ar/^{36}Ar$; (**b**) He isotopic compositions; (**c**) $^{3}He/^{4}He$ vs. $^{40}Ar^{*}/^{4}He$. Concentration of $^{40}Ar^{*}$ compared with the atmospheric $^{40}Ar/^{36}Ar$ = 296.0 was calculated by $^{40}Ar^{*} = (^{40}Ar/^{36}Ar - 296.0) \times {}^{36}Ar$; (**d**) Correlation diagram of $^{3}He/^{4}He$ vs. $^{4}He/^{40}Ar^{*}$, comparing the Thongkai-Ok hydrothermal fluid with selected magmatic- and formation water-derived ore fluids (modified from Kendrick and Burnard, 2013) [16]. The stars represent the mean mantle and crustal production ratios, and the rectangle box represents the range of crustal components.

The correlation diagram in Figure 4b shows the plotted data of ^{3}He versus ^{4}He distributed between the domains of crustal He and mantle He. This indicates a mixed fluid source of crustal and mantle origins. Additionally, the correlation diagrams $^{3}He/^{4}He$ (R/Ra) vs. $^{40}Ar/^{36}Ar$ (Figure 4a), $^{3}He/^{4}He$ vs. $^{40}Ar^{*}/^{4}He$ (Figure 4c), and $^{4}He/^{40}Ar^{*}$ vs. $^{3}He/^{4}He$ (Figure 4d), demonstrate that the ore-forming fluid can be interpreted as a combination of crustal and mantle components. Kendrick et al. (2001) [15] established the equation to estimate the mixing proportion of mantle and crustal components: the proportion of mantle $^{4}He = (R - R_c)/(R_m - R_c) \times 100\%$, where R_m: ~8.5, R_c: 0.01–0.05, and R: ~0.2 (the measured R/Ra of quartz separates samples from the Thongkai-Ok deposit). The calculated results indicate a proportion of mantle He in the ore-forming fluids of the Thongkai-Ok Au deposit of just ~2 percent.

Figure 5 shows heavy noble gas elemental ratios ($^{84}Kr/^{36}Ar$ and $^{132}Xe/^{36}Ar$) obtained with the crushing extraction. The data are plotted in the area accounted for by mixing between heavy noble gases dissolved in salt water (an average salinity of 3.0 wt% NaCl equivalent is assumed as revealed by the fluid inclusion study) at various temperatures and those derived from the atmosphere. The latter is "excess air", which was involved in the fluid as entrapment and dissolution of gas bubbles with atmospheric gas composition [36].

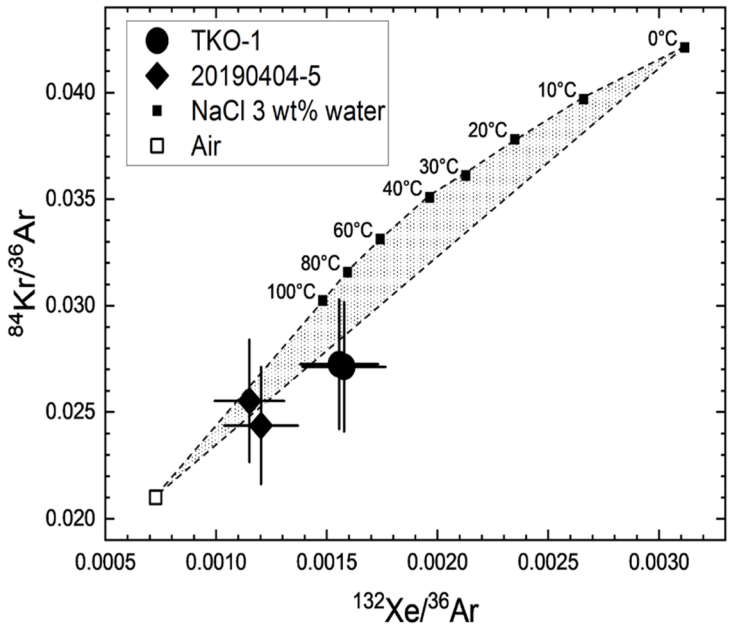

Figure 5. Plot of $^{84}Kr/^{36}Ar$ against $^{132}Xe/^{36}Ar$ obtained with crushing extraction. End-member compositions of air and air-saturated salt water (3.0 wt% NaCl equivalent) with temperatures ranging from 0 to 100 °C (calculated after Ballentine et al. (2002) [36]) are also plotted. A shaded area indicates a mixing between heavy noble gases dissolved in the salt water and unfractionated excess air. Error bars are 1 sigma.

If we assume the fluid in the quartz samples was derived from the 20 °C saltwater, approximately 30%–40% of ^{36}Ar extracted from the samples by the in vacuo crushing was contained in the salt water. Since the ^{36}Ar concentration in the 3.0 wt% NaCl equivalent salt water, which is in equilibrium with the atmosphere at 20 °C, is about 8.0×10^{-7} cm^3STP/g (calculated after Ballentine et al. (2002) [37]), the ^{36}Ar extracted from the samples by crushing (4.6×10^{-9} cm^3STP/g for 20190404-5 and 2.9×10^{-9} cm^3STP/g for TKO-1, respectively) would have been dissolved in ca 1.5–1.7 mg of the salt water. Assuming a crushing efficiency of 27%–30%, inferred from ^{3}He concentrations obtained by in vacuo crushing and powder fusion, about 5 mg of salt water was contained in 1 g of the sample quartz as fluid inclusions.

Although K concentration in the fluid is not well constrained, if we assume 2% of the 3.0 wt% NaCl equivalent salinity is from KCl as in seawater, K in the samples hosted by the fluid inclusions would be 6×10^{-5} % relative to the sample weight. This estimate is negligibly small compared to the bulk K content in the sample ranging from 0.046 to 0.059 wt% (Table 2). By comparison, crush-released (i.e., fluid inclusion-hosted) radiogenic ^{40}Ar is about 21%–24% of total radiogenic ^{40}Ar (Table 3), indicating that the extraordinary amount of excess Ar in the hydrothermal quartz from the Vangtat orogenic Au belt is predominantly concentrated in the fluid inclusions. Based on crush-released radiogenic ^{40}Ar (1.0×10^{-6} cm^3STP/g for 20190404-5 and TKO-1, respectively, Table 3) and 3.0 wt% NaCl equivalent salt water contents in the samples inferred from crush-released ^{36}Ar (1.5-1.7 mg), the excess Ar concentrations in the salt water are estimated to be 5.9–6.9×10^{-4} cm^3STP/g. This yields 5.1–6.1×10^{-5} of $^{40}Ar/Cl$ ratio of the salt water, which is in the range of those of metamorphic source fluids observed in quartz associated with cherts, granites, and sedimentary rocks [13,38,39]. This indicates that the hydrothermal fluid associated with the mineralized quartz veins at the Thongkai-Ok Au deposit [8] could have resulted in an "excess argon wave" similar to that suggested as the origin of excess Ar in the Sanbagawa eclogite [5].

8. Conclusions

This study involved the investigation of K-Ar and noble gas analysis on quartz separate samples from the Thongkai-Ok Au deposit in the Vangtat orogenic Au belt of southern Laos. The experimental results indicate that fluid inclusions inside quartz crystals in the mineralized quartz veins contained a large amount of radiogenic ^{40}Ar, which is known as the "excess Ar" that commonly affects K-Ar and/or Ar-Ar dating methods. Noble gas isotope ratios reveal that the Vangtat orogenic Au belt ore-forming fluid is mainly derived from a crustal component with a minor contribution of mantle origin.

Author Contributions: Conceptualization, A.A., P.B. and H.S.; formal analysis, P.B. and H.S.; field investigation, P.B. and A.A.; writing—original draft preparation, P.B.; writing—review and editing, H.S. and A.A.; funding acquisition, H.S. and A.A. All authors have read and agreed to the published version of the manuscript.

Funding: This study was supported by the Ken F. and Patricia Clark Fund at The University of Texas at El Paso and by the Japan International Corporation Agency (JICA).

Acknowledgments: Authors are highly indebted to Tetsumaru Itaya and Koshi Yagi of Okayama University of Sciences for their technical assistance with K-Ar analyses and insightful suggestions on this research and manuscript. The comments from two anonymous reviewers helped improve the manuscript.

Conflicts of Interest: The authors declare no conflict of interest.

References

1. Itaya, T. K-Ar phengite geochronology of HP-UHP metamorphic rocks-An in-depth review. *J. Miner. Petrol. Sci.* **2020**, *115*, 44–58. [CrossRef]
2. Wanless, R.K.; Stevens, R.D.; Loveridge, W.D. Anomalous parent-daughter isotopic relationships in rocks adjacent to the Grenville Front near Chibougamau, Quebec. *Eclogae Geol. Helv.* **1970**, *63*, 345–364.
3. Hyodo, H.; York, D. The discovery and significance of a fossilized radiogenic argon wave (argonami) in the earth's crust. *Geophys. Res. Lett.* **1993**, *20*, 61–64. [CrossRef]
4. Itaya, T.; Hyodo, H.; Tsujimori, T.; Wallis, S.; Aoya, M.; Kawakami, T.; Gouzu, C. Regional-Scale Excess Ar wave in a Barrovian type metamorphic belt, eastern Tibetan Plateau. *Isl. Arc.* **2009**, *18*, 293–305. [CrossRef]
5. Itaya, T.; Tsujimori, T. White mica K-Ar geochronology of the Sanbagawa eclogites in SW Japan: Implications on deformation-controlled K-Ar closure temperature. *Int. Geol. Rev.* **2005**, *57*, 1014–1022. [CrossRef]
6. Itaya, T.; Hyodo, H.; Uruno, K.; Mikoshiba, M.U. Ultra-high excess Argon in Kyanites: Implications for ultra-high pressure metamorphism in Northeast Japan. *Gondwana Res.* **2005**, *8*, 617–621. [CrossRef]
7. Itaya, T.; Yagi, K.; Gouzu, C.; Thanh, N.X.; Groppo, C. Preliminary report on the excess argon bearing K-feldspar from metagranite in the Brossasco-Isasca UHP Unit of Dora-Maira Massif, Italy. *J. Miner. Petrol. Sci.* **2017**, *112*, 36–39. [CrossRef]
8. Bounliyong, P.; Arribas, A.; Watanabe, Y.; Echigo, T.; Wong, H. A new orogenic gold belt in Southeast Asia: Geology, mineralogy, and genesis of the Vangtat gold deposit, Southeastern Laos. *Resour. Geol.* **2022**, *72*, e12283. [CrossRef]
9. Bounliyong, P.; Itaya, T.; Arribas, A.; Watanabe, Y.; Wong, H.; Echigo, T. K-Ar geochronology of orogenic gold mineralization in the Vangtat gold belt, southeastern Laos: Effect of excess argon in hydrothermal quartz. *Resour. Geol.* **2021**, *71*, 161–175. [CrossRef]
10. Rama, S.N.I.; Hart, S.R.; Roedder, E. Excess radiogenic argon in fluid inclusions. *J. Geophys. Res.* **1965**, *70*, 509–511. [CrossRef]
11. Kelley, S.; Turner, G.; Butterfield, A.; Shepherd, T.J. The source and significance of argon isotopes in fluid inclusions from areas of mineralization. *Earth Planet. Sci. Lett.* **1986**, *79*, 303–318. [CrossRef]
12. Wahler, W. Über die in Kristallen eingeschlossenen Flüssigkeiten und Gase. *Geochim. Cosmochim. Acta* **1956**, *9*, 105–135. (In German with English abstract). [CrossRef]
13. Turner, G.; Bannon, M.P. Argon isotope geochemistry of inclusion fluids from granite-associated mineral veins in southwest and northeast England. *Geochim. Cosmochim. Acta* **1992**, *56*, 227–243. [CrossRef]
14. Kelley, S. Excess argon in K–Ar and Ar-Ar geochronology. *Chem. Geol.* **2002**, *188*, 1–22. [CrossRef]
15. Kendrick, M.A.; Burgess, R.; Pattrick, R.A.D.; Turner, G. Fluid inclusion noble gas and halogen evidence on the origin of Cu-porphyry mineralising fluids. *Geochim. Cosmochim. Acta* **2001**, *65*, 2651–2668. [CrossRef]
16. Kendrick, M.A.; Burnard, P. Noble gases and halogens in fluid inclusions: A journey through the Earth's crust. In *The Noble Gases as Geochemical Tracers*; Burnard, P., Ed.; Springer: Berlin/Heidelberg, Germany, 2013; pp. 319–369.
17. Lepvrier, C.; Van Vuong, N.; Maluski, H.; Thi, P.T.; Van Vu, T. Indosinian tectonics in Vietnam. *C. R. Geoscience* **2008**, *340*, 94–111. [CrossRef]

18. Vilayhack, S.; Duangsurigna, S.; Voravong, A.; Vilaysan, P.; Khounchanthida, T.; Phommakaysone, K.; Goto, M.; Negishi, Y.; Tsuda, K.; Watanabe, Y.; et al. *1:200,000 Geological Map of B. Dakyoy with Report on Geology of B. Dakyoy District*; Japan International Cooperation Agency and Department of Geology, Ministry of Energy and Mines: Vientiane, Laos, 2008; pp. 1–44.
19. Lepvrier, C.; Maluski, H.; Van Tich, V.; Leyreloup, A.; Thi, P.T.; Van Vuong, N. The Early Triassic Indosinian orogeny in Vietnam (Truong Son Belt and Kontum Massif); implications for the geodynamic evolution of Indochina. *Tectonophysics* **2004**, *393*, 87–118. [CrossRef]
20. Osanai, Y.; Nakano, N.; Owada, M.; Miyamoto, T.; Nam, T.N.; Minh, N.T.; Nam, N.V.; Tri, T.V. Collision zone metamorphism in Vietnam and adjacent South-eastern Asia: Proposition for trans-Vietnam orogenic belt. *J. Miner. Petrol. Sci.* **2008**, *103*, 226–241. [CrossRef]
21. Manaka, T. A Study of Mineralogical, Geochemical and Geochronological Characteristics and Ore Genesis in Phuoc Son Gold Deposit Area, Central Vietnam. Ph.D. Thesis, ARC Centre of Excellence in Ore Deposits (CODES), University of Tasmania, Hobart, Australia, 2014; p. 285.
22. Tran, H.T.; Zaw, K.; Halpin, J.A.; Manaka, T.; Meffre, S.; Lai, C.K.; Lee, Y.; Van Le, H.; Dinh, S. The Tam Ky-Phuoc Son shear zone in Central Vietnam: Tectonic and metallogenic implications. *Gond. Res.* **2014**, *26*, 144–164. [CrossRef]
23. Roedder, E. Fluid inclusions. *Rev. Miner.* **1984**, *12*, 11–46.
24. Chi, G.; Diamond, L.W.; Lu, H.; Lai, J.; Chu, H. Common problems and pitfalls in fluid inclusion study: A review and discussion. *Minerals* **2020**, *11*, 7. [CrossRef]
25. Bodnar, R.J. Revised equation and table for determining the freezing point depression of H_2O-NaCl solutions. *Geochim. Cosmochim. Acta* **1993**, *57*, 683–684. [CrossRef]
26. Wilkinson, J.J. Fluid inclusions in hydrothermal ore deposits. *Lithos* **2001**, *55*, 229–272. [CrossRef]
27. Itaya, T.; Doi, M.; Ohira, T. Very low potassium analysis by flame photometry using ultra low blank chemical lines: An application of K-Ar method to ophiolites. *Geochem. J.* **1996**, *30*, 31–39. [CrossRef]
28. Itaya, T.; Nagao, K.; Inoue, K.; Honjou, Y.; Okada, T.; Ogata, A. Argon isotopic analysis by newly developed mass spectrometric system for K-Ar dating. *Miner. J.* **1991**, *15*, 203–221. [CrossRef]
29. Steiger, R.H.; Jager, E. Subcommission on Geochronology: Convention on the use of decay constants in geo- and cosmochronology. *Earth Planet. Sci. Lett.* **1977**, *36*, 359–362. [CrossRef]
30. Sumino, H.; Nagao, K.; Notsu, K. Highly sensitive and precise measurement of helium isotopes using a mass spectrometer with double collector system. *J-Stage* **2001**, *49*, 61–68. [CrossRef]
31. Matsuda, J.; Matsumoto, T.; Sumino, H.; Nagao, K.; Yamamoto, J.; Miura, Y.; Kaneoka, I.; Takahata, N.; Sano, Y. The $^3He/^4He$ ratio of the new internal He Standard of Japan (HESJ). *Geochem. J.* **2002**, *36*, 191–195. [CrossRef]
32. Ballentine, C.J.; Burnard, P.G. Production, release and transport of noble gases in the continental crust. *Rev. Minereal. Geochem.* **2002**, *47*, 481–538. [CrossRef]
33. Turner, G.; Burnard, P.; Ford, J.; Gilmour, J.D.; Lyon, I.C.; Stuart, F.M. Tracing fluid sources and interactions. *Philos. Trans. R. Soc. London Ser. A Phys. Eng. Sci.* **1993**, *344*, 127–140.
34. Stuart, F.M.; Burnard, P.G.; Taylor, R.E.A.; Turner, G. Resolving mantle and crustal contributions to ancient hydrothermal fluids: He-Ar isotopes in fluid inclusions from Dae Hwa W-Mo mineralisation, South Korea. *Geochim. Cosmochim. Acta* **1995**, *59*, 4663–4673. [CrossRef]
35. Burnard, P.G.; Hu, R.Z.; Turner, G.; Bi, X.W. Mantle, crustal and atmospheric noble gases in Ailaoshan gold deposits, Yunnan Province, China. *Geochim. Cosmochim. Acta* **1999**, *63*, 1595–1604. [CrossRef]
36. Heaton, T.; Vogel, J. "Excess air" in groundwater. *J. Hydrol.* **1981**, *50*, 201–216. [CrossRef]
37. Ballentine, C.J.; Burgess, R.; Marty, B. Tracing fluid origin, transport and interaction in the crust. *Rev. Miner. Geochem.* **2002**, *47*, 539–614. [CrossRef]
38. Turner, G. Hydrothermal fluids and argon isotopes in quartz veins and cherts. *Geochim. Cosmochim. Acta* **1988**, *52*, 1443–1448. [CrossRef]
39. Turner, G.; Songshan, W. Excess argon, crustal fluids and apparent isochrons from crushing K-feldspar. *Earth Planet. Sci. Lett.* **1992**, *110*, 193–211. [CrossRef]